

CFD-Based Three-Dimensional Turbofan Exhaust Nozzle Analysis System

B. D. Keith,* K. Uenishi,† and D. A. Dietrich‡
General Electric Aircraft Engines, Cincinnati, Ohio 45215

A three-dimensional turbofan exhaust nozzle analysis system based on computational fluid dynamics (CFD) has been developed. This system has been established to aid exhaust designers in the efficient assessment and screening of their design concepts, with the prospects of a reduction in both design cycle time and wind-tunnel test costs. A reliable CFD flow solver, user-friendly grid generator, and postprocessing software are included in the system. The system is easy to use for exhaust designers who are not particularly familiar with the inner workings of CFD. Validation and applicability studies have been performed using different exhaust nozzle configurations at on-design and off-design engine operating conditions. This work demonstrates that a CFD code integrated with automatic grid generation and postprocessing can be a useful analytical tool in the practical exhaust nozzle design process.

Nomenclature

M	= Mach number
P	= static pressure
P_A	= atmospheric static pressure
R	= radius
X	= axial station
X_{REF}	= reference length

Subscript

∞	= freestream conditions
----------	-------------------------

Introduction

Design Considerations

ACHIEVING an aerodynamic contour design that meets performance specifications for a modern high-bypass-ratio turbofan engine involves complex, time-consuming, and expensive analysis and testing. A great deal of this effort is expended in designing aerodynamic contours for the exhaust system components (fan nozzle, core nozzle, plug, etc.) that efficiently satisfy operating conditions of both on- and off-design conditions. The fundamental purpose of the exhaust system is to discharge the exhaust gases to the ambient pressure with the highest possible axial thrust at the cruise design condition. This requires exhaust designers to size the fan and core nozzle throats to ensure passage of the flow rate required by the engine cycle with minimum pressure loss and minimum external drag. In an actual design process, however, the mechanical constraints of the system may compromise the optimal aerodynamic shapes. A more detailed discussion of design issues associated with exhaust systems can be found in Ref. 1.

Figure 1 depicts the complete geometry of a typical turbofan engine including inlet, nacelle (fan cowl) and exhaust system (Fig. 1a), and of a simplified geometry of only the exhaust system configuration (Fig. 1b), which will be our main focus of this article. In addition, the exhaust system can be further

simplified to an axisymmetric geometry if upper and lower bifurcators and pylon are neglected. In this article, both axisymmetric and full three-dimensional analyses are considered. All test data configurations are three-dimensional.

Over the years, a large amount of time and budget has been consumed in testing exhaust systems as an integral part of the design process and as an aid in understanding the fundamental physics of exhaust flowfields. A typical exhaust flowfield of a powered nacelle consists of two or three streams having different total pressures and total temperatures, and includes significant regions of subsonic, transonic, and supersonic Mach numbers. In a typical design, weak shock waves occur on the core cowl and plug surfaces, which interact with the shear layer and the surface boundary layers (Fig. 2).

Furthermore, the installation of an exhaust system on an aircraft may have a significant impact on the exhaust system flowfield and performance. Present CFD capabilities have advanced to the point of being able to analyze flowfields of

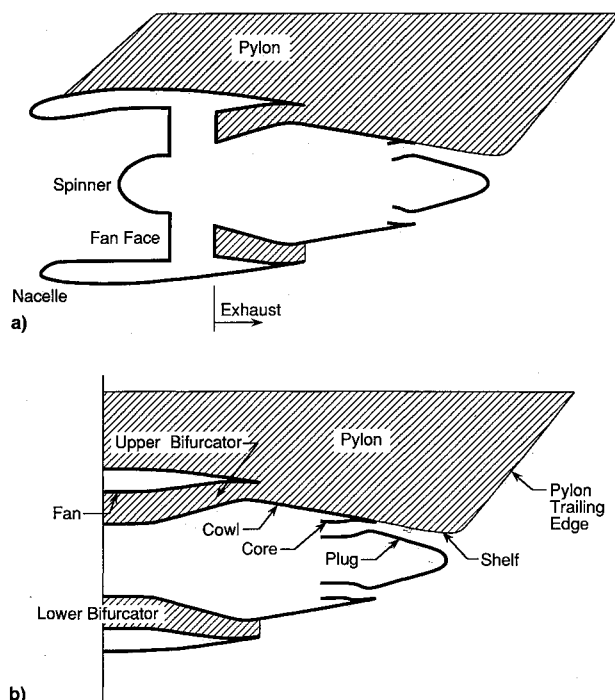


Fig. 1 Nacelle and exhaust aerodynamic components: a) complete geometry and b) exhaust-only components.

Presented as Paper 91-2478 at the AIAA/SAE/ASME 27th Joint Propulsion Conference, Sacramento, CA, June 24–26, 1991; received July 19, 1991; revision received Jan. 1, 1993; accepted for publication March 31, 1993. Copyright © 1991 by the American Institute of Aeronautics and Astronautics, Inc. All rights reserved.

*Engineer, Aero Systems Design.

†Staff Engineer, Aero Systems Design. Member AIAA.

‡Manager, Aero Systems Design. Member AIAA.

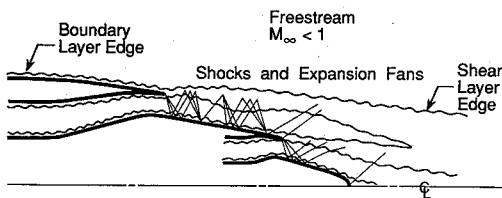


Fig. 2 Flowfield characteristics—turbofan exhaust system.

the installed exhaust systems under a wing. However, for the purpose of CFD applications to the exhaust system design, the current computational resources somewhat limit the analysis to the isolated exhaust system. The present work, therefore, is focused on the isolated exhaust design system. While the isolated analysis does not allow for determination of installation effects, it still allows evaluation of many nozzle design considerations, including 1) reduction of core cowl and plug shock strengths, 2) sizing of the throat areas, 3) friction drag, 4) suppression of the core flow, and 5) relative performance and discharge coefficient values.²

Computational Considerations

A relatively large number of analytical and computational methods for predicting flowfields surrounding a turbofan engine exhaust system have been developed.³⁻⁷ These methods include analytical/computational techniques based on two- and three-dimensional general Euler Navier-Stokes equations³⁻⁶ and Euler equations with shear layer wake mode.⁷ Even though these analytical and computational methods are well documented in general publications, they have not been fully transferred into or accepted by the design community due to the difficulties associated with grid generation, lack of systematic validation, and the requirements that the user possess specific CFD knowledge.

System Highlights

The objective of the present work has been the establishment of a CFD-based turbofan exhaust flowfield analysis system. The system can assist the designer in the evaluation and pretest screening of candidate designs quickly and efficiently and lead to a reduction in the total number of necessary test configurations. The main theme of this article is the description of a three-dimensional turbofan exhaust nozzle aerodynamic analysis system (ENS3D) developed to achieve the above mentioned objectives.

The ENS3D system can be applied either to a three-dimensional geometry which includes a pylon and lower bifurcator as shown in Fig. 1b, or to a simple axisymmetric configuration without considering the pylon and bifurcators. Since this system is to be used in the design environment, where the computational emphasis is on economic viability, the present study initially focused on the solution of the Euler equations. However, during the course of extensive validation studies, solutions based on Euler mode were found to be inadequate for exhaust system flowfields. The focus was shifted to establish the analyses based on viscous solutions with a simplified turbulence model applicable to the exhaust system flowfields.

In the following sections, major technical tasks in the development of a process for the analysis of three-dimensional turbofan exhaust configurations will be discussed: 1) selection and validation of a three-dimensional Navier Stokes solver; 2) development of an automated block-grid generator and postprocessing software for generic axisymmetric and three-dimensional exhaust systems; and 3) validation of the procedures using test data at various fan and core nozzle pressure ratios.

CFD Solver

In recent years, numerous CFD solvers aimed at solving generalized three-dimensional flowfields have been devel-

oped and shown to produce valid results. The CFL3D code was chosen as the base flow solver for the present work. References 8-12 contain the development details and examples of CFL3D-related work. CFL3D has the following attributes: 1) well demonstrated and documented applicability to three-dimensional complex problems; 2) use of modern numerical algorithms (implicit, upwinding, and finite volume scheme); and 3) multigrid capability with zonal and patched options. As described in Ref. 13, CFL3D has already demonstrated its success in the nacelle inlet/fan cowl design environment in terms of accuracy and efficiency.

The fundamental numerical schemes and governing equations used in CFL3D have been explicitly described in open publications⁸⁻¹²; therefore, this article will address only the specific aspects of CFL3D related to the modifications made for the implementation of the three-dimensional turbofan exhaust nozzle analysis system. Briefly, CFL3D solves the Euler or thin-layer Navier-Stokes equations using a well-known finite volume discretization method. Solutions are advanced in time with a spatially split three-factor approximate-factorization method in diagonalized form. Flux quantities are represented using the upwind-based flux-difference-splitting (FDS) approach of Roe, or the flux-vector-splitting (FVS) approach of van Leer, both with third-order spatial accuracy. Based upon numerous validation studies of specific turbofan exhaust systems and the previous inlet/fan cowl design system,⁸ van Leer's FVS method has proven to be more robust and efficient than Roe's FDS method without loss of accuracy. Despite criticisms of the FVS method,¹⁴ differences in results based on FVS and FDS are found to be very minor when applied to exhaust flows. Therefore, the robustness and efficiency without loss of accuracy make the FVS method a preferred approach in the design environment.

In the current ENS3D system, input to the CFL3D solver is dramatically reduced by presetting many of the available parameters and boundary conditions to proven values, and by coupling the solver to grid generation and postprocessing by routines for commonality and user-friendly implementation. The ENS3D system is currently optimized for execution in the viscous mode which incorporates a simple turbulence model for design applications.

As shown in Fig. 2, the exhaust flowfields contain two distinct turbulent flow characteristics: 1) shear layer/wake; and 2) boundary layer on the solid surfaces (i.e., core cowl, plug, fan and core duct surfaces, etc.). In order to model these turbulent flow phenomena accurately, high-order turbulence models are needed, which may not be consistent with the main goal of establishing a robust design CFD system.

It has been found that boundary-layer viscous effects strongly influence the exhaust near-field solution, which is of primary interest for the current study. The exhaust plume flowfield far downstream is, of course, dominated by the shear layer/wake viscous effect. But this has not been shown to have a dramatic effect on surface pressure distributions. More detailed discussion of these effects can be found in Ref. 14.

Therefore, in the current system, the standard Baldwin-Lomax turbulence model is used to model both viscous effects of the boundary layer and shear layer/wake, knowing that this model is not adequate for shear layer/wake modeling, but that the consequences are minimal, especially when considering surface pressure distributions. This simplified viscous model has predicted quite reasonable flowfields based on comparisons with test data, as will be shown later in this article.

Boundary Conditions

A typical isolated engine configuration includes the inlet, nacelle (fan cowl), fan-face, spinner, fan duct and core cowl, and core duct and plug, as shown in Fig. 1a. Since the primary interest of this work is to develop the analysis system for efficient exhaust nozzle aerodynamic design, the geometry can be simplified without loss of generality as shown in Fig. 1b. While the capabilities of the CFL3D solver are not limited

to this form of modeling, user-friendliness and computational costs have currently restricted ENS3D to using the model shown in Fig. 1b. ENS3D also includes the capability of analyzing axisymmetric flowfields, where existence of a pylon and bifurcators are neglected. An axisymmetric solution can accurately simulate flowfields away from a pylon or a bifurcator at considerably less time and cost, which will be shown in a later section. The boundary conditions used in ENS3D consist of far-field, solid surface (impermeable boundary), inflow for fan duct, core duct and freestream, and symmetric and axisymmetric planes. The original CFL3D code already possessed the far-field, solid surface, and symmetric boundary conditions, which are directly applied in ENS3D without modification. The far-field boundary condition is based on Riemann invariants for a one-dimensional flow.

On the solid surface the pressure and temperature gradients at a true normal to the surface are set to zero. For the Euler mode the velocity normal to the wall is set to zero and a slip condition is imposed. Conversely, nonslip conditions are imposed with the use of viscous analysis on all appropriate surfaces. The circumferential spacing of the grid does not allow for nonslip boundary conditions on the bifurcator or pylon side walls at current grid levels. The solid-surface condition is used for the walls of the core- and fan-ducts, core and fan cowl surfaces, plug surface, and pylon and bifurcator surfaces including the underside of the pylon shelf. For the three-dimensional analysis, a symmetric boundary condition is applied along the vertical plane of geometric symmetry, imparting a zero gradient, zero curvature boundary. For the axisymmetric mode, boundary conditions are imposed at $i = -5$ and $+5$ deg, that simulate an axisymmetric flowfield using only one cell in the circumferential direction. For the current turbofan exhaust configuration, the inflow boundaries of the fan and core ducts are always subsonic. Therefore, stagnation pressure, stagnation temperature, and flow angles are specified based on Riemann invariants, and the remaining flow properties are determined for the interior flowfield through numerical boundary conditions. These boundary conditions are specified in a general command file, also used to specify reference Reynold's number (viscous analysis), grid parameters, and convergence criteria. If total pressure and temperature profiles and swirl angle are desired, these values must then be specified for each cell center on the inlet plane.

Grid Generator

In establishing a three-dimensional, turbofan exhaust nozzle analysis system, it is critical to provide a grid generator that creates a grid suitable for complex geometries utilizing orthogonality and grid packing. In addition, the grid generator is required to be user friendly such that the system can be readily utilized by the design community, where modifications to an exhaust geometry may occur on a continuing basis. It is believed that both of these objectives have been met by the ENS3D grid generation package.

The primary geometry input for both axisymmetric and three-dimensional grids are the X and R coordinates for the external nacelle (fan cowl), fan duct outer wall and inner core cowl, and the core duct outer wall and inner plug. The current system is therefore restricted to axisymmetric nacelle shapes. This basic starting grid is shown in Fig. 3a, in the XR plane. When a three-dimensional grid is desired, the additional geometric definitions required include the X , R , and half-thickness for the lower bifurcator and upper bifurcator/pylon. Within the fan duct, the upper bifurcator/pylon is defined by stringer cuts running the length of the pylon at varying waterlines. For each point along the stringer, there is defined the axial station X , waterline value, and pylon half-thickness. Interpolations are then performed axially and radially to find the thickness at any radius. The lower bifurcator is similarly defined, and is restricted to the internal portion of the fan duct. An isometric view of the three-dimensional grid is shown in Fig. 3b.

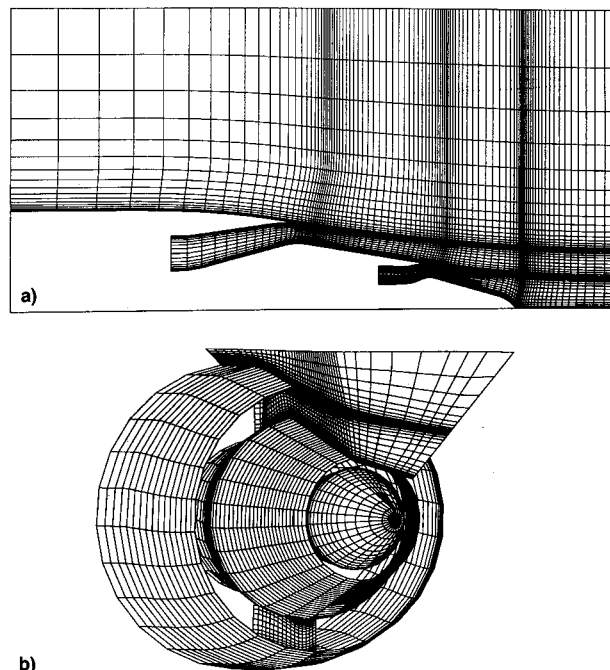


Fig. 3 Separate flow exhaust nozzle grid: a) XR planar grid and b) isometric view, three-dimensional surface grid.

When specifying an axisymmetric grid, the nozzle is gridded with one cell over a 10-deg wedge, the X , R grid points rotated to the $+5$ - and -5 -deg planes. When utilizing the three-dimensional capabilities, the grid is generated over the 180-deg half-plane. A variable number of circumferential grid cuts can be specified in this mode, and 13 have been used for the current study. Geometric specifications for the upper or lower bifurcator cause the grid to be rotated to the given thickness at that axial station. Therefore, the grid is skewed circumferentially due to these thicknesses as the planar grid is rotated to fit each of the desired cuts. The grid is also skewed axially in the region of the pylon as grid lines are forced to line up with the pylon trailing edge.

When a pylon shelf is present, an additional complication is introduced for the region of the core stream that lies underneath the shelf. To overcome this geometric problem, an additional grid block has been established in the core that provides a mesh for the flow in the region beneath the pylon shelf.

The resulting grids from this package are algebraic in nature. The grid is stretched in all directions by an exponential function which allows no more than 17% growth from cell i to $i + 1$. The grids can be run through a screening routine that will check for negative volumes. A typical grid for a viscous analysis had values of y^+ as low as four, with 14 grid lines in the boundary layer. Step size in the axial direction ranged from $\Delta X/\delta = 0.98$ to 4.3 near the throat where the boundary layer is thin.

Results and Discussion

The development of ENS3D as an analysis tool for separate flow turbofan exhausts progressed through a series of stages as its viability and modeling limitations for various flow conditions were studied. From the initial runs in the inviscid, axisymmetric mode it was evident that the CFL3D-based solver showed potential for accurately predicting exhaust surface pressures. The following discussion highlights many of the results obtained as the code progressed through several development stages.

Results are compared to data obtained from scale model testing of several representative turbofan exhaust systems. The data are proprietary and therefore not available to the general public as are the specifics of the geometry. All configurations used for this study are separate flow. In general,

data on external surfaces are provided at two circumferential locations, 40 and 185 deg, aft looking forward. These tests were conducted on both a static test stand (freestream Mach number = 0.0) as well as in a wind tunnel with cold flowing core and fan streams. Computational modeling required approximation of the static conditions with a freestream Mach number of 0.1 for numerical stability. It has been found that this small nonzero freestream Mach number does not adversely affect simulation of the static case. Analyzed flow conditions covered a range of pressure ratios for the fan and core streams with an approximate Reynolds number of 5.9×10^5 for the static case, 4.7×10^6 with freestream flow. The system is capable of analyzing flowfields modeled as any combination of 1) inviscid or viscous, 2) axisymmetric or three-dimensional, and 3) freestream static or flowing. The following material represents a cross section of the results to date.

Axisymmetric Analysis

Static

Typical results for the axisymmetric analyses are shown in Fig. 4, which includes test data for the following conditions:

- Fan nozzle pressure ratio (FNPR) = 2.4
- Core nozzle pressure ratio (CNPR) = 2.0
- Freestream Mach number = 0 (static test stand)

The ENS3D results for both inviscid and viscous modeling are indicated by the dashed and solid curves, respectively. Data and analytical results are shown for the fan duct, core cowl, core duct and plug. Several observations can be drawn from this analysis.

The axisymmetric analysis does not include the effects due to the blockage of any internal bifurcations. Since the test model included upper and lower bifurcation in the fan duct,

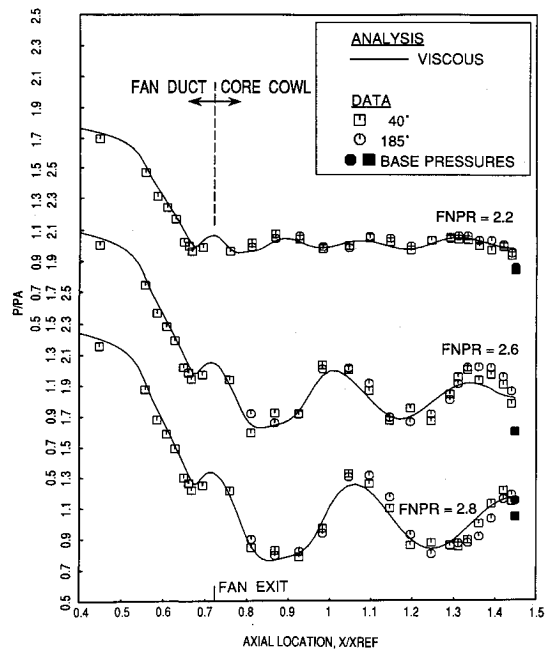


Fig. 5 Axisymmetric, viscous analyses for a range of fan pressure ratios—core cowl results, $M_\infty = 0.0$.

some differences between the data and analytical results should exist for regions upstream of the fan exit. As expected, Fig. 4a shows differences between the data and analysis in the fan duct, but very good agreement in the axisymmetric core duct (Fig. 4b).

One of the most significant regions for comparison of the data and analytical results is along the core cowl downstream of the fan exit and along the plug downstream of the core exit. As shown in Fig. 2, the flow along the exposed portions of the core cowl and plug can contain a series of expansion fans and shocks. Strong shocks in this region decrease engine performance, and this analysis technique can provide a means of reducing the strength of the shocks. Therefore, it is critical to model the flowfield accurately in these regions in order to adequately evaluate and design an exhaust system. In addition, the pressures at the base of the nacelle (fan cowl) and core cowl (regions where flowstreams intersect) are very important in order to obtain proper nozzle flow rates. The accuracy of matching the base pressure to data is highly dependent on the grid density in the vicinity of the base region. For a fixed number of grid points, some compromise between modeling of the transonic flow along the core cowl and plug and the modeling of the base region must be made. The current grid distribution seeks to maximize results along the core cowl. Redistribution of the same number of grid points to the exit regions will lead to better matching of base pressures to test data, but a loss in resolution along the remaining surfaces.

Figure 4 also shows the analytical results for the core cowl and plug surfaces as compared to experimental data. Note that the experimental data indicate some differences between the 40- and 185-deg locations, due in large part to the presence of an upper bifurcator and pylon in the test model. Since the analysis in this case is axisymmetric, the results cannot model any circumferential variation. Along the core cowl (Fig. 4a), comparison between the data and the inviscid results show that certain inadequacies are evident in the inviscid solution. First, the axial locations of the minimum and maximum pressures are not accurate. Second, the inviscid solution does not contain damping of the pressure profile that is evident in the test data. In the case of the viscous analysis, the grid density has been increased in the vicinity of the solid walls and shear layers, and the solver has been executed using the Baldwin-Lomax mixing length model for turbulent flow. A comparison

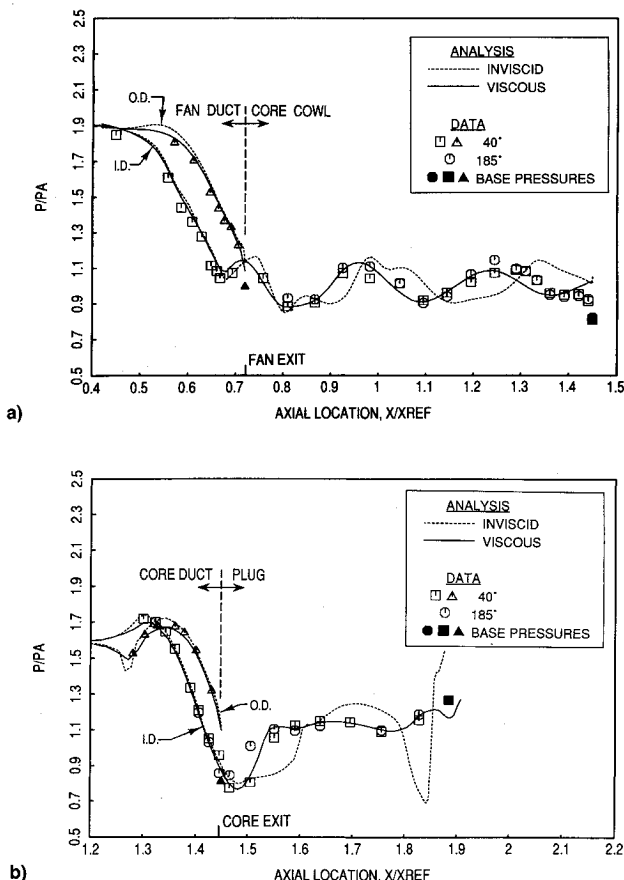
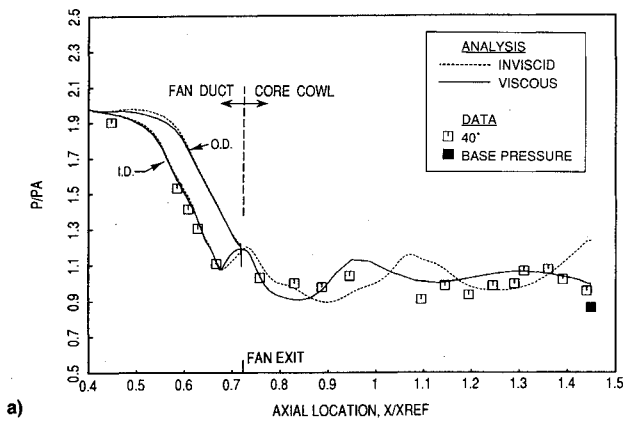
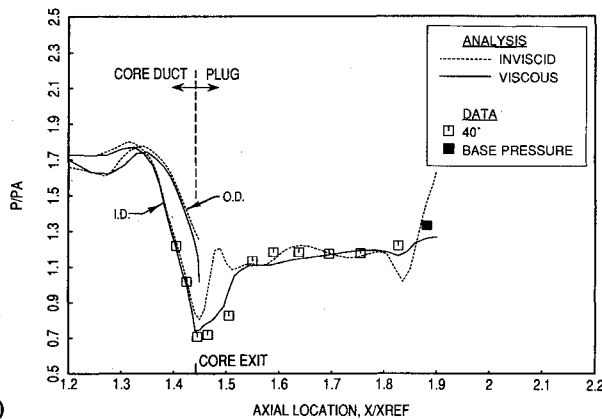


Fig. 4 Axisymmetric analysis vs data, $M_\infty = 0.0$, fan nozzle pressure ratio = 2.4, core nozzle pressure ratio = 2.0: a) fan duct and core cowl and b) core duct and plug.



a)



b)

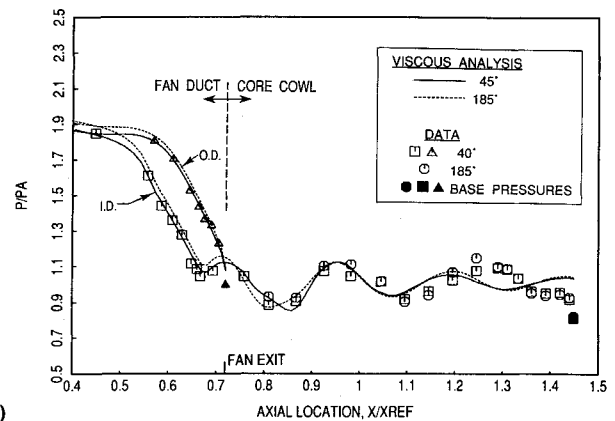
Fig. 6 Axisymmetric analysis vs data, $M_\infty = 0.8$, fan nozzle pressure ratio = 2.4, core nozzle pressure ratio = 2.0: a) fan duct and core cowl and b) core duct and plug.

between the test data and the viscous results indicates that the core cowl pressure distribution, including the location of the expansion/compression waves and the damping, is accurately modeled. The viscous solution clearly represents a more accurate model of the flowfield when compared to the inviscid results.

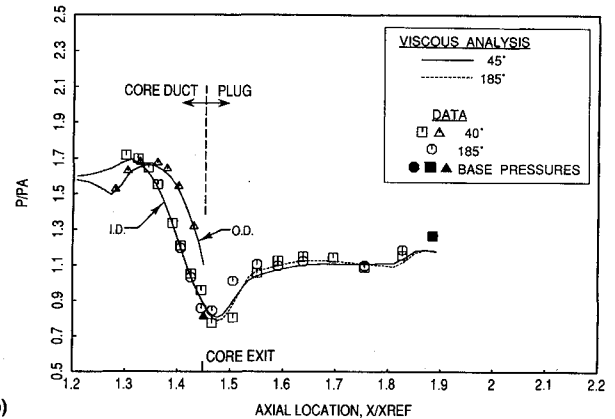
Turning to the plug surface (Fig. 4b), the inadequacy of the inviscid solution in matching the pressure distribution along the plug surface is clearly evident. Note the extreme over-expansion and recompression as the plug is closed out. The viscous solution, however, does show excellent agreement with the test data. As in the above discussion concerning the core cowl, the number and distribution of the grid points differ between the inviscid and viscous solutions. Certainly, the detailed differences in any grid definition and the method used to model viscous effects would have a bearing on the accuracy of any solution. However, it appears from this work that the flowfield within and about a separate flow exhaust system can be accurately modeled, particularly if viscous effects are taken into account. Having test data prior to analysis allows for an examination of various grid densities to best match the data. This experience will then have to be utilized as the user moves on to similar geometries and flow conditions where data are not available. This will establish the kind of y^+ and $\Delta X/\delta$ values that are necessary for a quality solution.

Figure 5 shows a comparison of experimental pressure distributions to the analytical results of axisymmetric viscous solutions for a range of fan nozzle pressure ratios. The data shown in the figure are restricted to the core cowl only for clarity. The comparison of the test data and analytical results shows excellent agreement for all of the pressure ratios and illustrates the accuracy of matching the expansion/compression waves along the core cowl.

Regarding computational costs, this solver was run on a Cray YMP8/464. Viscous, axisymmetric solutions with 50,000



a)



b)

Fig. 7 Viscous three-dimensional analysis vs data, $M_\infty = 0.0$, fan nozzle pressure ratio = 2.4, core nozzle pressure ratio = 2.0: a) fan duct and core cowl and b) core duct and plug.

grid points over five grid blocks required 21 CPU minutes from an initial run, reaching a peak CFL number of 15 and using approximately 1000 time steps; utilizing the restart function reduced this to 11 CPU minutes (approximately 500 time steps) for additional cases with the same number of grid points. Convergence is established after no further reductions in CFL number are evident and the pressure distributions have stabilized. These criteria provide a viable level of computational time for use in the design process.

Freestream Flow

The operation of a turbofan exhaust system includes flight conditions over a range of freestream Mach numbers. Figure 6 compares the results of an axisymmetric ENS3D analysis to experimental data for a freestream Mach number of 0.8. Analytic results for both inviscid and viscous methods are shown in the figure. The experimental data have been obtained from an isolated, sting mounted exhaust system in a wind tunnel, where freestream flow can be simulated. Even with the exhaust system having reduced pressure instrumentation relative to previous comparisons, the accuracy of the technique and the impact of viscous modeling can be determined. When freestream flow is included, there are viscous effects both along the wall surfaces and within the shear layers. Figure 6 illustrates that the viscous modeling is more accurate than inviscid modeling in matching the expansion/compression waves along the core cowl, the base pressure on the core cowl, and the pressure distribution along the plug. In particular, the inviscid model resulted in an extremely high core cowl base pressure (Fig. 6a) leading to suppression of the core flow, as seen by the inviscid pressure distribution in the region of the core exit (Fig. 6b).

The inability of the viscous solution to match data along the core cowl with the accuracy demonstrated by the static freestream cases would be an indication of the shortcoming

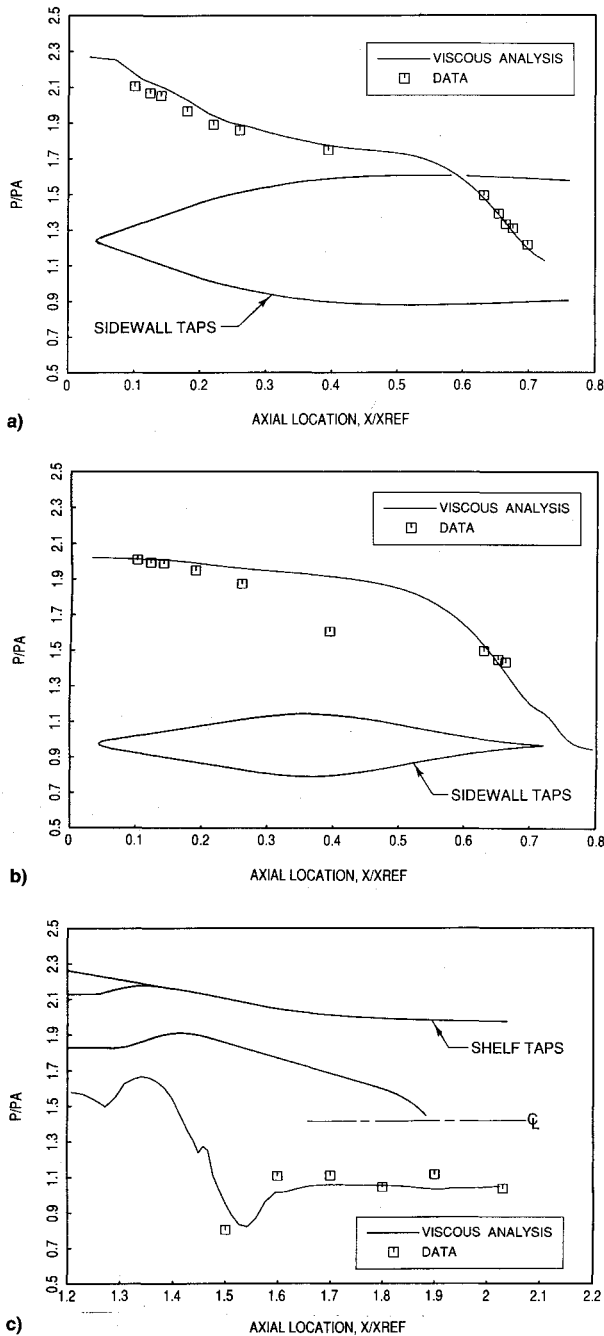


Fig. 8 Viscous three-dimensional analysis vs data, $M_\infty = 0.0$, fan nozzle pressure ratio = 2.4, core nozzle pressure ratio = 2.0: a) upper bifurcator, b) lower bifurcator, and c) shelf.

of the Baldwin-Lomax model as applied to shear layers. Until this issue is resolved, there will be several limitations on the effectiveness of installed calculations where there is also free-stream flow. However, since the performance guarantees are based on static tests, the current system will be helpful in improving nozzle performance.

Three-Dimensional Analysis

As mentioned previously, the ENS3D system is capable of performing both axisymmetric and fully three-dimensional analyses. As noted in Fig. 1b, the three-dimensional nature of the flowfield is introduced by the presence of upper and lower bifurcations, pylon, and shelf. Figure 7 presents the results of a three-dimensional viscous analysis and the associated experimental data for the static case previously discussed. There is slightly better agreement in the fan duct than the axisymmetric analysis provided, especially in the upstream

regions where the bifurcators most effect the flow. Along the core cowl, the analysis fails to demonstrate any ability to substantially differentiate the circumferential variations in pressure due to the bifurcators and pylon. There is good general agreement with data, but the results do not greatly enhance the axisymmetric results already obtained. Where the analysis does surpass axisymmetric results is in the ability to examine pressure distributions along such three-dimensional features as the upper and lower bifurcator sidewalls and the shelf underside. Comparisons with data for these surfaces are shown in Fig. 8.

Computational constraints have limited the grid to 13 cuts over the 180-deg half-plane. Viscous, three-dimensional solutions were run with 325,000 grid points distributed over seven blocks and required 140 CPU minutes from an initial run, 67 minutes from restart. Again, these analyses had a peak CFL number of 15, and required approximately 1000 iterations for the initial run, 500 from restart. Circumferential variations may be better modeled if additional cuts can be incorporated into the grid.

Summary

A three-dimensional turbofan exhaust nozzle analysis system has been presented. Based on the CFL3D solver, this system provides grid generation capabilities for axisymmetric or three-dimensional configurations, and solves the flowfield in either the inviscid or viscous mode. As the results indicate, the viscous mode, utilizing the Baldwin-Lomax turbulence model, greatly enhances the solution accuracy. Axisymmetric results are very representative of the exhaust flowfield in regions away from the influence of bifurcators and the pylon; the three-dimensional analysis adds the capability of resolving pressure distributions along the bifurcator, pylon, and shelf surfaces. Ease of use and accuracy of results should prove the system to be an asset to the exhaust designer. Any progress relative to the three-dimensional solution will require additional grid in the circumferential direction, greatly increasing computational costs. A higher order turbulence model would help the solutions for the wind on case, but add a higher level of complexity and a reduction in robustness.

References

- Lahti, D. J., Dietrich, D. A., Stockman, N. M. O., and Faust, G. K., "Application of Computational Methods to the Design of Large Turbofan Engine Nacelles," AIAA Paper 84-0121, Jan. 1984.
- Abdol-Hamid, K. S., Uenishi, K., Carlson, J. R., and Keith, B. D., "Commercial Turbofan Engine Exhaust Nozzle Flow Analysis Using PAB3D," *Journal of Propulsion and Power*, Vol. 9, No. 3, 1993, pp. 431-436.
- Peery, K. M., and Forester, C. K., "Numerical Simulation of Multistream Nozzle Flows," AIAA Paper 79-1549, July 1979.
- Kreskovsky, J. P., Briley, W. R., and McDonald, H., "Investigation of Mixing in a Turbofan Exhaust Duct, Part I: Analysis and Computational Procedure," *AIAA Journal*, Vol. 22, No. 3, 1984, pp. 374-382.
- Chen, H. C., Kusuho, K., and Yu, N. J., "Flow Simulations for Detailed Nacelle—Exhaust Flow Using Euler Equations," AIAA Paper 85-5003, Oct. 1985.
- Brown, J. J., "A Nozzle Design Analysis Technique," AIAA Paper 86-1613, June 1986.
- Peace, A. J., "A Method for Calculating Axisymmetric Afterbody Flows," *Journal of Propulsion and Power*, Vol. 13, No. 4, 1987, pp. 357-364.
- Thomas, J. L., Van Leer, B., and Walters, R. W., "Implicit Flux-Split Schemes for the Euler Equations," AIAA Paper 85-1680, July 1985.
- Thomas, J. L., and Newsome, R. W., "Navier-Stokes Computations of Lee-Side Flows over Delta Wings," AIAA Paper 86-1049, May 1986.
- Anderson, W. K., Thomas, J. L., and Whitfield, D. L., "Multigrid Acceleration of the Flux-Split Euler Equations," *AIAA Jour-*

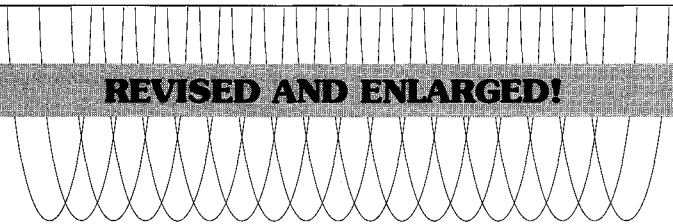
nal, Vol. 26, No. 6, 1988, pp. 649-654.

¹¹Ghaffari, F., Bates, B., Luckring, J., and Thomas, J. L. "Navier-Stokes Solutions About the F/A-18 Forebody-LEX Configurations," AIAA Paper 80-0338, Jan. 1989.

¹²Van Leer, B., Thomas, J. L., Roe, P. L., and Newsome, R. W., "A Comparison of Numerical Flux Formulas for the Euler and Navier-Stokes Equations," AIAA Paper 87-1104, June 1987.

¹³Uenishi, K., Pearson, M. S., Lehnig, T. R., and Leon, R. M., "Computational Fluid Dynamics Based Three-Dimensional Turbofan Inlet/Fan Cowl Analysis System," *Journal of Propulsion and Power*, Vol. 8, No. 1, 1992, pp. 175-183.

¹⁴Abdol-Hamid, K. S., Uenishi, K., and Turner, W. M., "A Three-Dimensional Upwinding Navier-Stokes Code with *k*-Model for Supersonic Flow," AIAA Paper 91-1669, June 1991.



REVISED AND ENLARGED!

AIAA Aerospace Design Engineers Guide

Third Edition

This third, revised and enlarged edition provides a condensed collection of commonly used engineering reference data specifically related to aerospace design. It's an essential tool for every design engineer!

TABLE OF CONTENTS:

Mathematics • Section properties • Conversion factors • Structural elements • Mechanical design
Electrical/electronic • Aircraft design • Earth, sea and solar system • Materials and specifications
Spacecraft design • Geometric dimensioning and tolerancing

**1993, 294 pp, illus, 9 x 3 1/8" leather-tone wire binding, ISBN 1-56347-045-4
AIAA Members \$ 29.95, Nonmembers \$49.95, Order #: 45-4(945)**

Place your order today! Call 1-800/682-AIAA



American Institute of Aeronautics and Astronautics

Publications Customer Service, 9 Jay Gould Ct., P.O. Box 753, Waldorf, MD 20604
FAX 301/843-0159 Phone 1-800/682-2422 9 a.m. - 5 p.m. Eastern

Sales Tax: CA residents, 8.25%; DC, 6%. For shipping and handling add \$4.75 for 1-4 books (call for rates for higher quantities). Orders under \$100.00 must be prepaid. Foreign orders must be prepaid and include a \$20.00 postal surcharge. Please allow 4 weeks for delivery. Prices are subject to change without notice. Returns will be accepted within 30 days. Non-U.S. residents are responsible for payment of any taxes required by their government.